Int. J. Environ. Sci. Technol. (2015) 12:3351–3362
DOI 10.1007/s13762-015-0762-9

ORIGINAL PAPER

# Biosorption characteristics of 1,8-dihydroxy anthraquinone onto *Aspergillus oryzae* CGMCC5992 biomass

**Z. Zhang · D. Shi · H. Ding · H. Zheng · H. Chen**

Received: 6 June 2014 / Revised: 9 January 2015 / Accepted: 14 January 2015 / Published online: 24 January 2015


**Abstract** 1,8-Dihydroxy anthraquinone is the intermediate usually used in the dye and pharmaceutical industry, and its direct discharge into water results in serious pollution. In the present study, we aimed to remove 1,8-dihydroxy anthraquinone and investigate its biosorption mechanism of anthraquinone onto nonviable *Aspergillus oryzae* CGMCC5992 biomass. Biosorption data were intuitively described by Langmuir isotherm and the pseudo-second-order kinetic model. According to the Langmuir model, it deduced that the maximum biosorption capacity of 1,8-dihydroxy anthraquinone was 62.82 mg $g^{-1}$ at 30 °C and pH 3.0. Characterization of the interaction between biosorbent and possible dye-biosorbent was further confirmed by Fourier transform infrared spectroscopy and scanning electron microscopy. Experimental results suggested that *A. oryzae* biomass as low-cost, environmentally friendly and efficient biosorbent could be successfully employed in the removal of 1,8-dihydroxy anthraquinone from aqueous solution.

**Keywords** *Aspergillus oryzae* CGMCC5992 · 1,8-Dihydroxy anthraquinone · Biosorption · Kinetics · Isotherms

Z. Zhang · D. Shi · H. Ding
School of Food Science and Biotechnology, Jiangsu University, Zhenjiang 212013, People's Republic of China

Z. Zhang (✉)
Institute of Agr-Production Processing Engineering, Jiangsu University, Xuefu Road 301, Zhenjiang 212013, People's Republic of China
e-mail: zhangtamei@163.com

H. Zheng · H. Chen
Jiangsu Alphay Bio-technology Co. Ltd., Nantong 226009, People's Republic of China

## Introduction

Over one million tons of organic dyes are produced annually, and more than 50,000 tons are lost in effluents during the application and manufacturing. 5–15 % of lost organic dyes are directly discharged into the natural environment (Carmen and Daniela 2012). The anthraquinone-containing wastewater is the second largest amount effluents in the field of commercial trichromatic dyes (Epolito et al. 2005). As a type of frequently used dye intermediates, anthraquinone (Fig. 1) threatens the survival of aquatic species and human health due to its typical structure of mental pollution (Chequer et al. 2011). It is imperative to remove anthraquinone pollutants from the wastewater before discharging it into major water bodies. However, it is not easy to oxidize anthraquinone dye in wastewater due to its low solubility, stable property and poor biodegradability. How to remove a small amount of anthraquinone dye in wastewater has become a key issue of environmental security.

Many methods are available to remove organic pollutants from wastewater. These methods can be mainly divided into physical processes (Rauf et al. 2008; Nasuha et al. 2010; Gupta et al. 2011a, b, 2013), chemical processes (Hua et al. 2013; Kalsoom et al. 2012), physical–chemical processes (Gupta and Nayak 2012), photocatalytic processes (Gupta et al. 2011a, b, 2012) and electrochemical processes (del Río et al. 2009; Ahmed Basha et al. 2012; Tsantaki et al. 2012). However, few methods can be extensively applied due to low efficiency, special equipment requirement, high treatment cost and generation of secondary pollution problems, such as the sludge, wastewater, solid residual and so on, which require further treatments (Saratale et al. 2011).

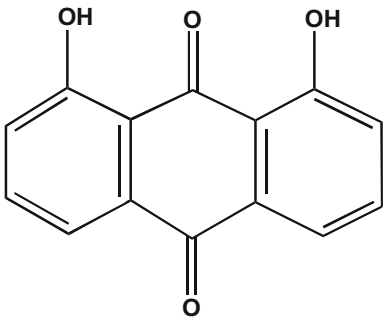


**Fig. 1** The chemical structure of 1,8-dihydroxy anthraquinone

In recent years, the biological treatment technology, especially low-cost alternative adsorbents of biomass (LCAs), has attracted more interest because of its high effectiveness, lower cost, less sludge production, environmental friendliness and suitableness for large-scale applications (Gupta and Suhas 2009; Freitas et al. 2009). The key step in the bio-treatment of wastewater is to discover the strains which can rapidly and effectively degrade organic materials (Meng et al. 2014). Extensive studies showed that *Phanerochaete chrysosporium* possesses a stronger ability to degrade pyrene (Wang et al. 2014), lignin (Zeng et al. 2013; Vincent et al. 2014) and other refractory organics compared with other strains, such as *Aspergillus nidulans* (Xi et al. 2013), *Pseudomonas putida* (Caro et al. 2008) and *Pantoea agglomerans* (Bhatia and Sharma 2010). However, this strain cannot degrade the recalcitrant compounds, such as anthraquinone pollutants in the effluent medium with limited carbon and nitrogen sources (Bosco et al. 1996; Hormiga et al. 2008; Peng et al. 2014). Therefore, it is necessary to explore efficient strains for the biotreatment of dyes effluents.

In our previous study, we showed that *A. oryzae* CGMCC5992 isolated from sludge in the Yudai River of Jiangsu University (Zhenjiang, China) can effectively degrade organic materials in the vinasse and reduce the COD from 4,600 to 323 mg $L^{-1}$ (Zhang et al. 2013). *A. oryzae* CGMCC5992 as a safe strain certified by US Food and Drug Administration also has a short culture cycle (28 °C, 2 days) and high yield (300 g $L^{-1}$ wet biomass). It can produce more crucial materials [manganese peroxidase (MnP) and lignin peroxidase (LiP)] for the degradation of recalcitrant compounds in high concentrations of gallic acid. The biomass of *A. oryzae* can effectively adsorb gallic acid, exhibiting an excellent removal rate of 99.21 % (Zhang et al. 2014).These results revealed that *A. oryzae* has unique advantages to degrade recalcitrant compounds.

In the present study, we used biomass of *A. oryzae* to adsorb 1,8-dihydroxy anthraquinone in the wastewater. The adsorption mechanism of anthraquinone compounds was studied by analyzing the adsorption kinetics and equilibrium of 1,8-dihydroxy anthraquinone onto *A. oryzae biomass*. The treated wastewater with 1,8-dihydroxy anthraquinone (<2 mg $L^{-1}$), total sugar content (<8.7 mg $L^{-1}$), total protein content (<5.3 mg $L^{-1}$) and total chemical oxygen demand (<150 mg $L^{-1}$) met the local wastewater discharge standard. Moreover, this technique could be applied in the industrial treatment of anthraquinone dye wastewater in the future.

## Materials and methods

### Microorganisms and chemicals

*A. oryzae* CGMCC5992 was isolated from the sludge of the Yudai River at Jiangsu University and stored in the China General Microbiological Culture Collection Center. It was cultured on the potato dextrose agar (PDA) slants at 28 °C for 4 days, then stored at 4 °C, and passaged every 7–9 weeks. All of the chemical reagents used in our present study were of analytical grades.

### Preparation of 1,8-dihydroxy anthraquinone solution

Briefly, 0.1000*g* 1,8-dihydroxy anthraquinone was completely dissolved in 1.0 mL ethanol. Then the solution was diluted to 1,000 mL with distilled water and ultrasonically dispersed until a uniform solution was obtained, which was used as the 1,8-dihydroxy anthraquinone stock solution and properly diluted according to experimental requirement prior to further analysis.

### Preparation of biomass of *A. oryzae* CGMCC5992

A 250-mL Erlenmeyer flask containing 100 mL potato dextrose medium was sterilized at 121 °C for 30 min. After the flask was cooled down to room temperature, 0.1 mL suspension containing $1 \times 10^6$ spores from the strain slants was aseptically inoculated into the flasks. The flasks were incubated in a reciprocating thermal-controlled air-bath shaker at 28 °C, 150 rpm for 2 days. The biomass was obtained from the broth through filtration with four layers of gauze, washed with sterile water for three times, and then stored at 4 °C prior to further analysis. The live biomass was sterilized at 121 °C for 20 min to obtain the dead biomass.

### Adsorption experiments

Adsorption experiments were carried out with a 250-mL Erlenmeyer flask containing 100 mL dye solution in a reciprocating thermal-controlled air-bath shaker at 125 rpm and 30 °C. Various concentrations of 1,8-

dihydroxy anthraquinone and different doses of biomass were added to each flask. After adsorption for 1 h, 1-mL sample was taken to measure residual dye concentrations. Except for the test in the pH effect on the adsorption, the pH of 1,8-dihydroxy anthraquinone solutions in other tests was adjusted to 6.5.

The analysis of adsorption kinetics was carried out in a 250-mL Erlenmeyer flask containing 100 mL 100 mg $L^{-1}$ 1,8-dihydroxy anthraquinone. In the process of adsorption, samples were taken out at 5, 10, 20, 30, 60 and 90 min, respectively, to determine the residual concentration of 1,8-dihydroxy anthraquinone. To obtain adsorption isotherms, the adsorption was carried out at 30 °C in a 250-mL flask containing 1,8-dihydroxy anthraquinone of initial concentrations at 10, 20, 40, 60, 80, 100 mg $L^{-1}$, respectively. After absorption equilibrium by 0.2 g biomass, the residual concentration of 1,8-dihydroxy anthraquinone was determined.

The adsorption capability ($q_e$) of adsorbent and the removal rate ($R_e$) of 1,8-dihydroxy anthraquinone by the biomass were calculated according to equations as follows:

$$q_e = \frac{(C_0 - C)V}{M} \quad (1)$$

$$R_e = \frac{C_0 - C_t}{C_0} \times 100\% \quad (2)$$

where $C_0$ and $C_t$ represent initial and equilibrium concentrations, respectively (mg $L^{-1}$). $C_t$ is the dye concentration (mg $L^{-1}$) after the adsorption procedure. $V$ is the volume of the solution in liter (L), and $M$ is the mass of the adsorbent (g).

## Analytical methods

### *Analysis of biomass*

The fungal growth was determined by measuring the dry weight of the cells. The fermentation broth was filtered with sterile carbasus. The residue was collected and washed by water until a colorless solution was obtained, and then dried at 105 °C to a constant weight. Finally, dry weight was determined by analytical balance.

The moisture content of the biomass ($w$) was calculated according to following equation:

$$w = \frac{M_0 - m}{M_0} \times 100\ \% \quad (3)$$

where $m$ and $M_0$ represent dry weight and wet weight, respectively.

### *Analysis of 1,8-dihydroxy anthraquinone content*

The content of 1,8-dihydro anthraquinone in the aqueous solution was analyzed using a HPLC system (Himadzu LC-20 AT Pump, N2000 station, USA) equipped with a UV detector. The analysis was performed on C18 column (4.6 mm × 250 mm × 5 μm, pore size of 100 Å, Australia). The mobile phase was 85 % methanol containing 0.1 % phosphonic acid, and the flow rate was set up at 0.8 mL $min^{-1}$. Moreover, the 1,8-dihydroxy anthraquinone content was determined based on the absorbance at a wavelength of 500 nm. The 1,8-dihydroxy anthraquinone peak in sample was confirmed using standard of 1,8-dihydroxy anthraquinone, and the content of 1,8-dihydroxy anthraquinone was calculated using the external standard method.

### *Data analysis*

All the experiments in this study were carried out in triplicate, and the results were expressed as mean ± SEs.

## Characterization of the biosorbent

### *Fourier transform infrared spectroscopy (FTIR)*

FTIR was performed using a ThermoFisher Nicolet FT-IR spectrometer (USA) in a region of 650–4,000 $cm^{-1}$ with a resolution of 4 $cm^{-1}$. The samples were ground and pressed into KBr pellets for analysis. Spectra of the adsorbent before and after the sorption were recorded.

### *Scanning electron microscopy (SEM) observation of biomass*

The morphological properties of the biosorbent before and after the adsorption of 1,8-dihydroxy anthraquinone were examined by a Hitachi S-4800 microscope (Japan).

# Results and discussion

## Comparison of the adsorption effect with live and dead biomass of *A. oryzae*

Figure 2 shows the removal rate of 1,8-dihydroxy anthraquinone by live and dead biomass of *A. oryzae* at different time points in the process of adsorption. The removal of dead biomass was far lower than that of living biomass. Many previous studies have reported that the group is involved in adsorption from the macromolecule, such as protein, polysaccharide and usually exists on surface of cell wall and membrane (Ostolska and Wiśniewska 2014; Ettelaie and Akinshina 2014). The high temperature inactivated the biomass, resulting in the macromolecules involved in adsorption denaturation. After denaturation, these molecules were changed from the regular spatial

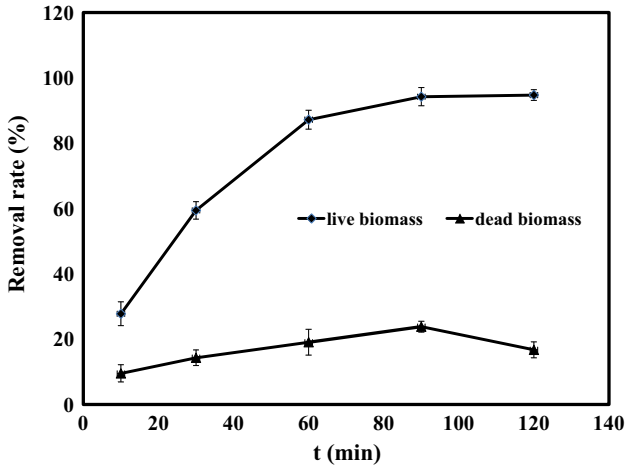


**Fig. 2** The different adsorption capacity of live and dead biomass of *A. oryzae* (pH 6.5, temperature 28 °C, biomass dose 2 g $L^{-1}$, initial dye concentration 100 mg $L^{-1}$, shaking speed 125 rpm)

structure to irregular coil structure and some groups in these macromolecules were involved in adsorption hinds from outer of molecules to inner of molecules. These changes cumbered the adsorption effect of *A. oryzae* biomass. The removal rate of 1,8-dihydroxy anthraquinone was 23.81 % at 90 min using the dead biomass as adsorbent, and it was far lower than that using live biomass as adsorbent (94.21 % at 90 min). Therefore, live biomass was selected in further experiments.

## Effect of pH on biosorption

The pH of an aqueous solution affects the ionization degree of the adsorbent involved in adsorption and the dye molecules (Plazinski 2013). Moreover, pH is closely related to changes in the structural stability and color intensity of the dye molecule (Saeed et al. 2010). In the present study, the pH of 1,8-dihydroxy anthraquinone solutions was adjusted to 1.0, 2.0, 3.0, 4.0, 5.0, 6.0 and 7.0 using 1 mol $L^{-1}$ HCl or 1 mol $L^{-1}$ NaOH, respectively. Figure 3a shows that the removal rate of 1,8-dihydroxy anthraquinone was increased from 84.8 to 97.68 % when the pH was increased from 1 to 3 in the adsorption process. When pH is less than 3.0, the hydroxyl group in the molecule is not ionized and the molecule is uncharged. The bio-macromolecules, such as proteins, usually possess an isoelectric point (Tamara et al. 2015; Tavolaro et al. 2009), at which pH a particular molecule carries no net electrical charge. When the pH of solution is lower or higher than the isoelectric point, the molecule is charged. When the pH of solution was less than 3.0, the 1,8-dihydroxy anthraquinone was uncharged, but the biomass was charged. The adsorption effect between the 1,8-dihydroxy anthraquinone and biomass was weak. Therefore, the removal rate of 1,8-dihydroxy anthraquinone was less than 97.68 % (at pH 3.0). When pH was higher than 3.0, the two hydroxyl groups of 1,8-dihydroxy anthraquinone involved in adsorption were ionized and the 1,8-dihydroxy anthraquinone molecules carried negative charge, so the adsorption effect was decreased, and the removal rate of 1,8-dihydroxy anthraquinone was reduced.

## Effect of contact time on biosorption

In the adsorption process, the contact time between the adsorbate and adsorbent plays a significantly important role in the practical application (Xi et al. 2013). Figure 3b shows the effect of different adsorption time on the removal rate of 0.1 mg $mL^{-1}$ 1,8-dihydroxy anthraquinone solution by live biomass (2.0 g $L^{-1}$). The adsorption profile of 1,8-dihydroxy anthraquinone could be divided into three stages according to our findings. The first stage included the initial 30 min, with a trait that the adsorbate was rapidly adsorbed and the removal rate was linearly increased. The second stage was from 30 to 90 min, with a trait that the variation of adsorption rate of 1,8-dihydroxy anthraquinone was decreased in several steps. The third stage was after 90 min, with a trait that the adsorption reached the equilibrium, and the removal rate of 1,8-dihydroxy anthraquinone remained stationary in this stage. These three stages have been extensively reported in literature (Zafar et al. 2008). Furthermore, the first stage may last from several minutes to a few hours, while the slow one may continue from several hours to a day (Saeed et al. 2009). The first stage is probably due to the abundant availability of adsorption sites on the adsorbent, whereas the adsorption process becomes less efficient since these sites are gradually occupied during the second stage (Iqbal and Saeed 2007). The biosorption curves are single and continuous leading to saturation, indicating the possible monolayer coverage of the adsorbate molecules on the adsorbent surface (Senthil Kumar et al. 2010).

## Effect of temperature on biosorption

The effects of temperature on the adsorption rate of biomass were investigated at 15, 20, 25, 30, 35 and 40 °C. Figure 3c shows that the adsorption rate was increased with the temperature from 15 to 30 °C, and the maximum removal rate of 99.13 % was observed at 30 °C. When the temperature was higher than 30 °C, a decrease in removal rate indicated that this biosorption process was exothermic, and the physical bonding between the adsorbate molecules and adsorbents was weakened with the increase in temperature.

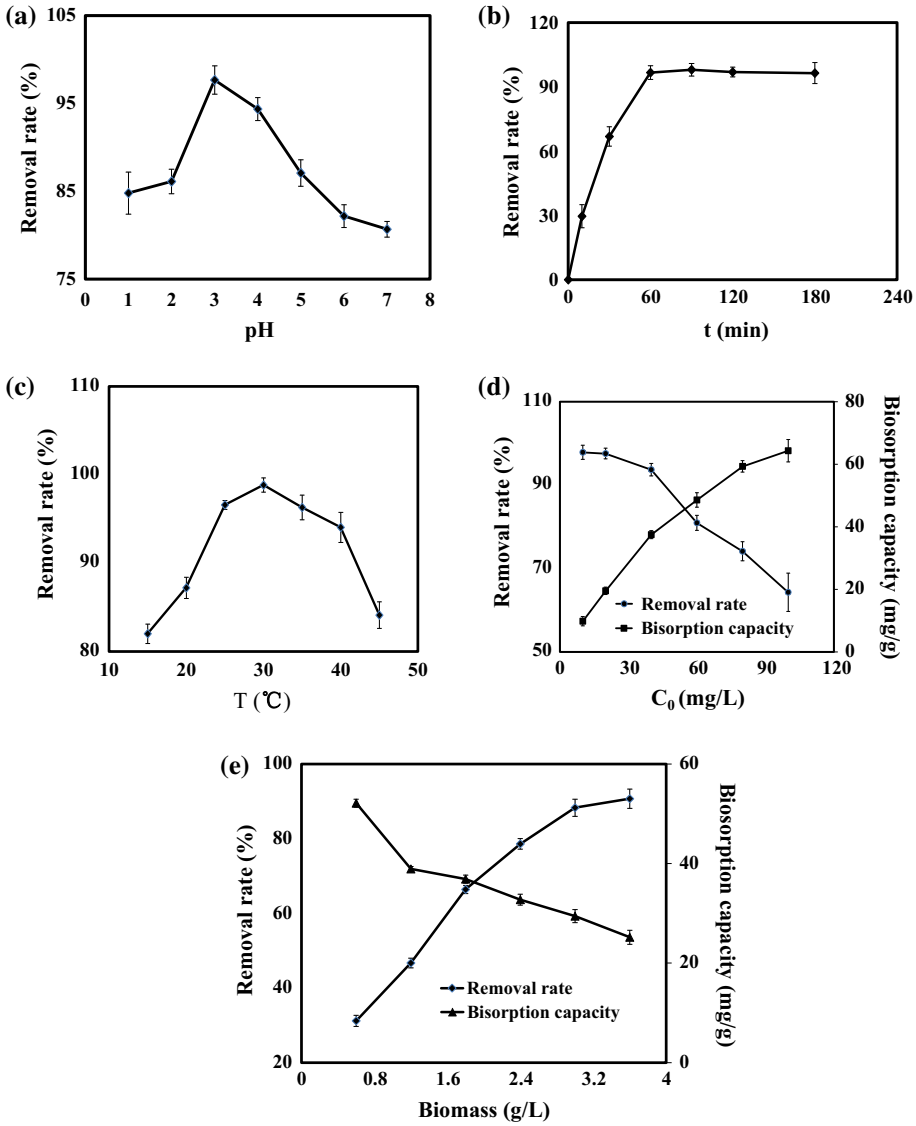


**Fig. 3** Effects of pH (**a**) (contact time 60 min, temperature 28 °C, biomass dose 2 g $L^{-1}$, $C_0$ = 100 mg $L^{-1}$, shaking speed 125 rpm); contact time (**b**) (pH 3.0, temperature 28 °C, biomass dose 2 g $L^{-1}$, $C_0$ = 100 mg $L^{-1}$, shaking speed 125 rpm); temperature (**c**) (contact time 60 min, pH 3.0, biomass dose 2 g $L^{-1}$, $C_0$ = 100 mg $L^{-1}$, shaking speed 125 rpm); initial dye concentration (**d**) (contact time 60 min, pH 3.0, temperature 30 °C, biomass dose 1 g $L^{-1}$, shaking speed 125 rpm); initial biomass concentration (**e**) (contact time 60 min, pH 3.0, temperature 30 °C, $C_0$ = 100 mg $L^{-1}$, shaking speed 125 rpm)

## Effect of initial 1,8-dihydroxy anthraquinone concentration on biosorption

The biosorption process is greatly affected by the initial concentration of the adsorbate (Saha et al. 2012). Figure 3d shows the removal rate of 1,8-dihydroxy anthraquinone and biosorption amount for live biomass at different initial adsorbate concentrations (10–100 mg $L^{-1}$). The biosorption amount for live biomass of *A. oryzae* was rapidly increased with the increase in initial concentration of 1,8-dihydroxy anthraquinone. Arica and Bayramoglu have reported similar results (Arica and Bayramoglu 2007). A liquid film exists between the aqueous phase and the adsorbent (Chowdhury et al. 2011). The adsorption process can be described as some consecutive steps starting with liquid film diffusion, internal diffusion and adsorption of solute on the interior surfaces of the pores and capillary space of the sorbent. The last step is relatively fast (Marungrueng and Pavasant 2007). The biosorption of 1,8-dihydroxy anthraquinone onto the active biomass of *A. oryzae* may be governed by the film diffusion process. There is a difference in adsorbate concentrations between the exterior and interior of the liquid film due to adsorption, and such a difference of the absorbate concentration drives the film diffusion process. When the concentration of adsorbate in the inner side of the film is near 0 mg $L^{-1}$ due to the adsorption at the beginning of adsorption, the impetus of the adsorption depends on the outer side of the film. At this time, the concentration of the adsorbate in the outer side of the film was higher, and the impetus was greater (Akkaya and Özer 2005). Although the adsorption amount was increased, the removal rate was decreased from 97.80 to 62.48 % with the increase in the initial adsorbate concentration. All adsorbate molecules in the

**Table 1** Parameters of pseudo-first-order and pseudo-second-order kinetics models

| $T$ ( °C) | $q_{e,exp}$ (mg $g^{-1}$) | Pseudo-first-order constants | | | Pseudo-second-order constants | | |
|---|---|---|---|---|---|---|---|
| | | $K_1$ ($min^{-1}$) | $q_{e,1}$ (mg $g^{-1}$) | $R^2$ | $K_2$ (g $mg^{-1}$ $min^{-1}$) | $q_{e,2}$ (mg $g^{-1}$) | $R^2$ |
| 20 | 41.35 | 0.02993 | 32.96 | 0.907 | 0.00271 | 41.67 | 0.999 |
| 30 | 66.12 | 0.02503 | 14.13 | 0.944 | 0.00833 | 66.67 | 0.999 |
| 40 | 55.28 | 0.02321 | 21.24 | 0.908 | 0.00368 | 55.56 | 0.998 |
| 50 | 51.83 | 0.02623 | 27.10 | 0.965 | 0.00284 | 52.63 | 0.999 |

solution can interact with the adsorption sites of the biosorbent at lower concentrations. However, a certain amount of adsorbents only have a limited number of adsorption sites. When these sites are occupied with adsorbates, the adsorbent could not adsorb any adsorbates. Therefore, the high initial concentration of 1,8-dihydroxy anthraquinone resulted in a decreased removal rate.

### Effect of the live biomass amount of *A. oryzae* on biosorption

Figure 3e shows the effect of the live biomass amount of *A. oryzae* on the removal rate and biosorption amount of 1,8-dihydroxy anthraquinone. When the biomass amount was increased from 0.6 to 3.0 g $L^{-1}$, the removal rate of 1,8-dihydroxy anthraquinone was linearly increased from 31.2 to 88.3 %, whereas the adsorption amount of live biomass was decreased from 52.3 to 29.4 mg $g^{-1}$. The increase in the removal rate of 1,8-dihydroxy anthraquinone could be explained by the increased surface area and available adsorption sites of the adsorbent (Akar et al. 2009). However, the removal rate of 1,8-dihydroxy anthraquinone was not increased with the increase in biomass amount from 3.0 to 3.6 g $L^{-1}$. This could be explained by that all adsorbate molecules bind onto adsorbent surface, and no extra adsorbate molecules bind to the redundant absorbents (Bhattacharyya and Sharma 2004).

### Kinetic modeling of experimental data

To examine the controlling mechanism of the adsorption process, such as mass transfer and chemical reaction, the pseudo-first-order and the pseudo-second-order kinetics models were used to analyze the experimental data of dye adsorption by live biomass.

#### *Pseudo-first-order model*

The linear pseudo-first-order model is generally expressed as follows (Lorenc-Grabowska et al. 2013):

$$\log(q_e - q_t) = \log q_e - k_1 \times \frac{t}{2.303} \quad (4)$$

where $q_t$ (mg $g^{-1}$) and $q_e$ (mg $g^{-1}$) are the amounts of 1,8-dihydroxy anthraquinone adsorbed on live biomass at time $t$ (min) and equilibrium, respectively, and $k_1$ ($min^{-1}$) is the rate constant of pseudo-first-order adsorption. The $q_e$ and $k_1$ can be calculated from the slope and intercept by plotting $log\ (q_e - q_t)$ versus t.

#### *Pseudo-second-order model*

The linear pseudo-second-order model is generally expressed as following equation: (Ho and McKay 2000):

$$\frac{t}{q_t} = \frac{1}{K_2 q_e^2} + \frac{t}{q_e} \quad (5)$$

where $K_2$ (g $mg^{-1}$ $min^{-1}$) is the rate constant of pseudo-second-order adsorption. The $q_e$ and $k_2$ can be calculated from the slope and intercept by plotting $t/q_t$ versus t.

#### *Inference from kinetic modeling equations*

The experimental data for the removal rate of 1,8-dihydroxy anthraquinone were modeled using the pseudo-first-order equation (Eq. 4) and pseudo-second-order equation (Eq. 5), respectively. Table 1 shows the kinetic parameters. The equilibrium biosorption capacity $q_e$ values obtained, respectively, from calculation and experiment are consistent at different temperatures (Table 1). It is clear that the equilibrium capacity $q_e$ at 30 °C was higher than that of other temperatures. We found that the value of $R^2$ fitted by the pseudo-first-order equation for all temperature levels was less than 0.97 and less than that fitted by the pseudo-second-order equation for all temperature levels which were near or equal to 0.99. These results suggested that the biosorption of 1,8-dihydroxy anthraquinone by live biomass of *A. oryzae* could be well fitted by the pseudo-second-order kinetics. Without involvement in any biological process, the dead mycelia adsorption should be the sole role of physical–chemical interaction (Huang et al. 2010). The adsorption of 1,8-dihydroxy anthraquinone by living mycelia cells, however, was more diverse and possibly involved both biological adsorption and surface active reactions (Gulnaz

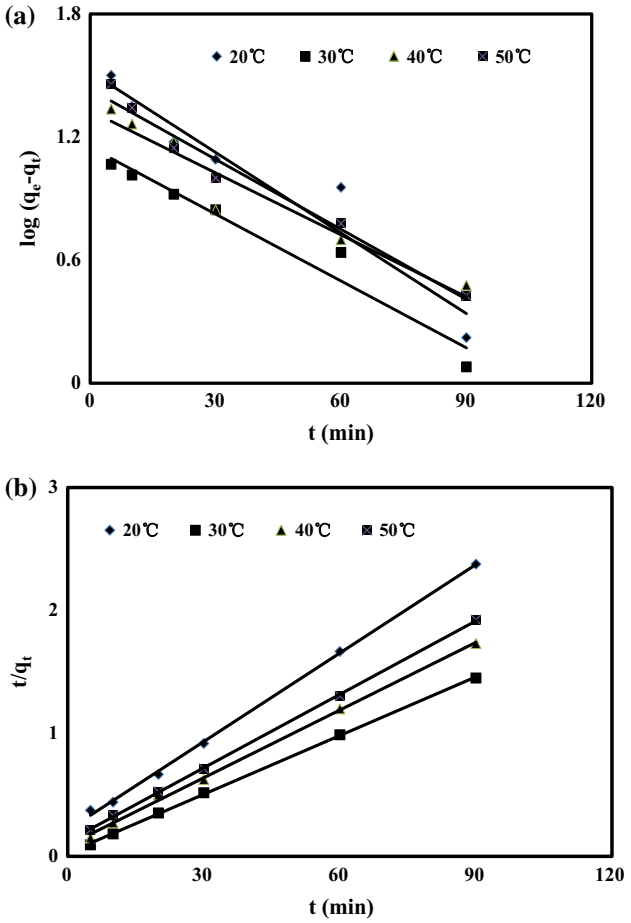


**Fig. 4** Pseudo-first-order kinetic plot (**a**) and Pseudo-second-order kinetic plot (**b**) for the adsorption of 1,8-dihydroxy anthraquinone onto biomass ($C_0$ = 100 mg $L^{-1}$, biomass dose 2 g $L^{-1}$, pH 3.0, temperature 30 °C, shaking speed 125 rpm)

et al. 2006; El Haddad et al. 2014). The reviews showed that (in most cases) the pseudo-second order equation is able to correlate with the measured kinetic sorption isotherms well. Moreover, it almost always appears to be better applicable than the pseudo-first-order equation (Plazinski 2013). These characters and reviews also supported our findings. Compared with Fig. 4b, the pseudo-second-order model clearly displayed a quite linear curve over the entire range of the experimental values.

## Adsorption isotherm

There are several adsorption isotherms fitting the adsorption process based on different adsorption mechanisms. Among those, the Langmuir and Freundlich models are widely used for modeling the adsorption on activated sludge, such as estrogens (Ren et al. 2007), dyes (Li et al. 2011) and heavy metals (Ibrahim 2011). Therefore, both above-mentioned isotherms were applied in our present study.

### *Langmuir model*

The Langmuir model assumes that the adsorption takes place in the monolayer form at specific homogeneous sites within the biosorbent. The linear form is expressed as follows (Gupta et al. 2011a, b):

$$\frac{1}{q_e} = \frac{1}{Q_0} + \frac{1}{bQ_0C_e} \tag{6}$$

where $Q_0$ and $b$ are Langmuir constants, corresponding to maximum adsorption capacity at complete monolayer coverage (mg $g^{-1}$) and equilibrium constant (L $mg^{-1}$), respectively. $C_e$ (mg $L^{-1}$) is the adsorbate concentration in the aqueous phase at equilibrium. The values of $b$ and $Q_0$ can be calculated from the intercept and slope by plotting $1/q_e$ versus $1/C_e$ (Fig. 5a).

The essential trait of the Langmuir isotherm can be expressed by the equilibrium parameter $R_L$, which indicates the favorability of the adsorption process. The values of $R_L$ were calculated according the equation as follows:

$$R_L = \frac{1}{1 + bC_0} \tag{7}$$

where $C_0$ is the highest initial adsorbate concentration (mg $L^{-1}$). The type of the isotherm can be classified according to values of the separation factor as follows: $R_L > 1$: unfavorable isotherm; $R_L = 1$: linear isotherm; $0 < R_L < 1$: favorable isotherm; $R_L = 0$: irreversible isotherm (Jain et al. 2010).

### *Freundlich model*

The Freundlich model expresses the uptake of adsorbate on a heterogeneous surface of the adsorbent. The equation form is expressed as follows:

$$\log q_e = \log K_f + \frac{1}{n}\log C_e \tag{8}$$

where $K_f$ and $n$ are Freundlich isotherm constants. They can be calculated from the intercept and slope by plotting log $q_e$ versus log $C_e$ (Fig. 5b).

### *Inference from isotherm modeling equations*

The Langmuir model is based on the assumption that the adsorption takes place in the monolayer form at specific homogeneous sites within the biosorbent, where all the adsorption sites are identical and energetically equivalent, and no further adsorption can take place at the site once an adsorbate molecule occupies this site (Monash and Pugazhenthi 2009). The intermolecular forces are rapidly decreased with the increase in distance, and consequently, the existence of monolayer coverage of the adsorbate at the outer surface of the adsorbent can be predicted. The

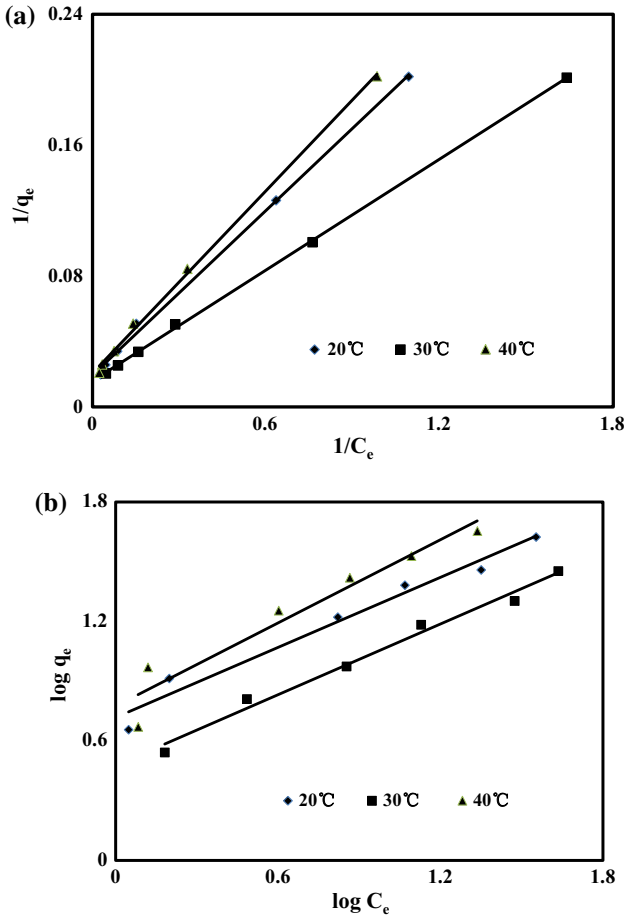


**Fig. 5** Langmuir isotherm (**a**) and Freundlich isotherm (**b**) of the adsorption of 1,8-dihydroxy anthraquinone onto biomass (contact time 60 min, $C_0$ = 10–100 mg $L^{-1}$, biomass dose 2 g $L^{-1}$, pH 3.0, temperature 30 °C, shaking speed 125 rpm)

Freundlich isotherm model is an empirical expression, including the heterogeneity of the surface and the exponential distribution of sites and their energies.

The equilibrium parameter $R_L$ of the Langmuir model was in the range of 0–1, and the value of $n$ of the Freundlich model was in the range of 1–10 (Table 2). The $R_L$ and $n$ all indicated the favorable adsorption of 1,8-dihydroxy anthraquinone on live biomass of *A. oryzae* (Günay et al. 2007). The correlation coefficients from the Langmuir model fitting (>0.99) showed that the Langmuir model could better describe the experimental data, suggesting that it was more suitable for modeling 1,8-dihydroxy anthraquinone on live biomass of *A. oryzae*. This result indicated that the adsorption of 1,8-dihydroxy anthraquinone occurred at single layer, and the adsorption sites were homogeneously distributed on the surface of live biomass of *A. oryzae* (Li et al. 2013).

## Characterization of live biomass of *A. oryzae* surfaces

Figure 6 shows that the biomass changed from loose structure to tight structure after the adsorption of 1,8-dihydroxy anthraquinone, and the color of biomass changed from colorless to earth yellow.

SEM was used to examine micro- and ultrastructural changes on the surface of live biomass of *A. oryzae* before and after the biosorption process (Fig. 7). The biosorbent without adsorbing the 1,8-dihydroxy anthraquinone displayed a plicate and porous surface structure (Fig. 7a, c). Porous structure provides more adsorption sites and increases contact area and pore diffusion during the adsorption process (Pang et al. 2011). Figure 7b, d indicates that the 1,8-dihydroxy anthraquinone molecules were trapped and adsorbed into these pores.

## FTIR analysis

FTIR spectroscopy is a powerful method to assess the chemical environment of the biomaterial responsible for adsorption (Xiao et al. 2014). Figure 8 shows representative FTIR records of the biomass of *A. oryzae* untreated and treated with 1,8-dihydroxy anthraquinone within a wavelength range of 4,000–650 $cm^{-1}$ under ambient conditions. The analysis of FTIR records of untreated and treated samples reflected the complex nature of the live biomass.

In general, the FTIR spectra of all the fungal preparations exhibited intense peaks at a frequency level of 3,400–3,200 $cm^{-1}$, representing stretching of –OH groups and –NH groups (Pang et al. 2011). A significant change can be observed, for the broad and strong band in the case at 3,294 $cm^{-1}$, indicating the presence of bond hydroxyl groups (–OH) or amine (–NH) groups, which was shifted to

**Table 2** The Langmuir and Freundlich model parameters of 1,8-dihydroxy anthraquinone adsorption on biomass pellets at different temperatures

| $T$(°C) | Langmuir isotherm | | | | Freundlich isotherm | | |
|---|---|---|---|---|---|---|---|
| | $Q_0$ (mg $g^{-1}$) | $b$ (L $mg^{-1}$) | $R_L$ | $R^2$ | $K_f$ (mg $g^{-1}$) | $n$ (g $L^{-1}$) | $R^2$ |
| 20 | 51.28 | 0.0792 | 0.1168 | 0.997 | 5.223 | 1.709 | 0.964 |
| 30 | 62.82 | 0.0663 | 0.0984 | 0.999 | 6.966 | 1.587 | 0.971 |
| 40 | 48.31 | 0.0824 | 0.1213 | 0.997 | 2.998 | 1.695 | 0.982 |

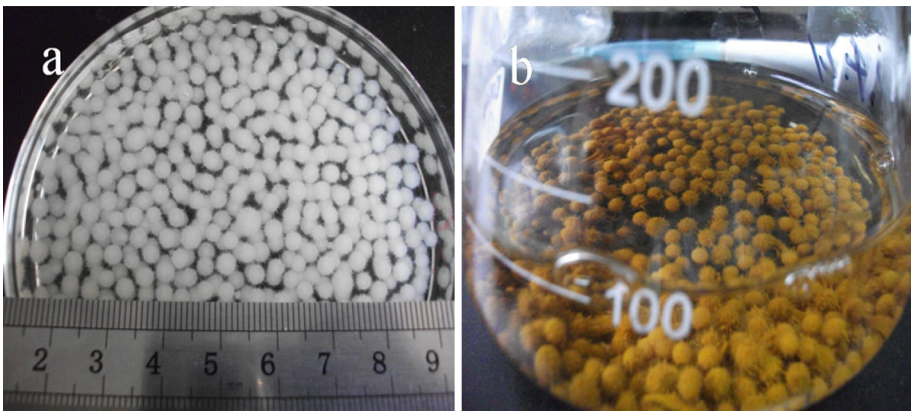


**Fig. 6** The live biomass of *A. oryzae* before adsorption (**a**) and after adsorption (**b**)

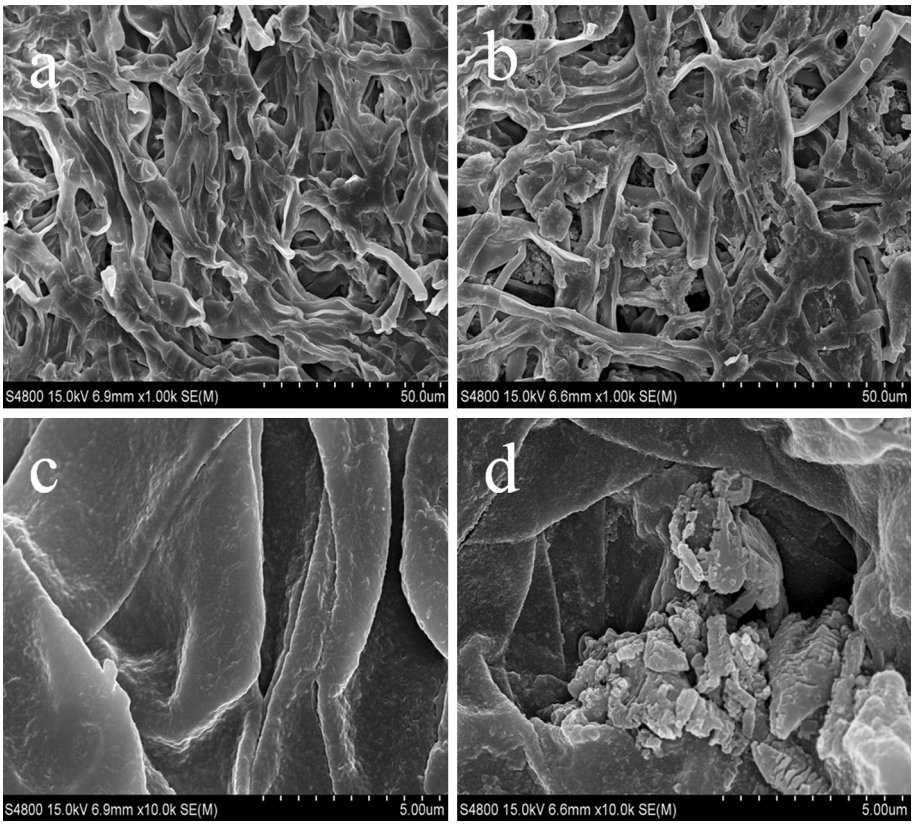


**Fig. 7** SEM photographs of biomass before (**a**, **c**) and after (**b**, **d**) 1,8-dihydroxy anthraquinone adsorption

3,323 $cm^{-1}$ ($\triangle\upsilon = 29\ cm^{-1}$) after biosorption of 1,8-dihydroxy anthraquinone (Nagy et al. 2013). The bands observed near 1,630 $cm^{-1}$ indicated the fingerprint region of C=O, C–O and O–H that exist as functional groups of live biomass of *A. oryzae*. The bands in the region 1,640–1,450 $cm^{-1}$ can be ascribed to the C=C stretching vibrations in the aromatic ring bands (Vučurović et al. 2014). The peak at 1,642.98, 1,546.98 and 1,312.21 $cm^{-1}$ in unloaded biomass shifted to 1,626.71, 1,466.75 and 1,281.72 $cm^{-1}$ on 1,8-dihydroxy anthraquinone-loaded biomass, respectively. The peak at 1,123.42 $cm^{-1}$ disappeared. The shifting or disappearance of these bands might be due to the functional groups of biosorbents, which combined with groups of 1,8-dihydroxy anthraquinone and formed new chemical bonds. These observations indicated the involvement of these functional groups (C=O, O–H, N–H, C–H et al.) in the biosorption process (Akar et al. 2005). After the adsorption of 1,8-dihydroxy anthraquinone onto live biomass of *A. oryzae* surface, significant changes in the FTIR spectra were observed and those surface functional groups were responsible for 1,8-dihydroxy anthraquinone uptake capacity of adsorbents (Shahul Hameed et al. 2013).

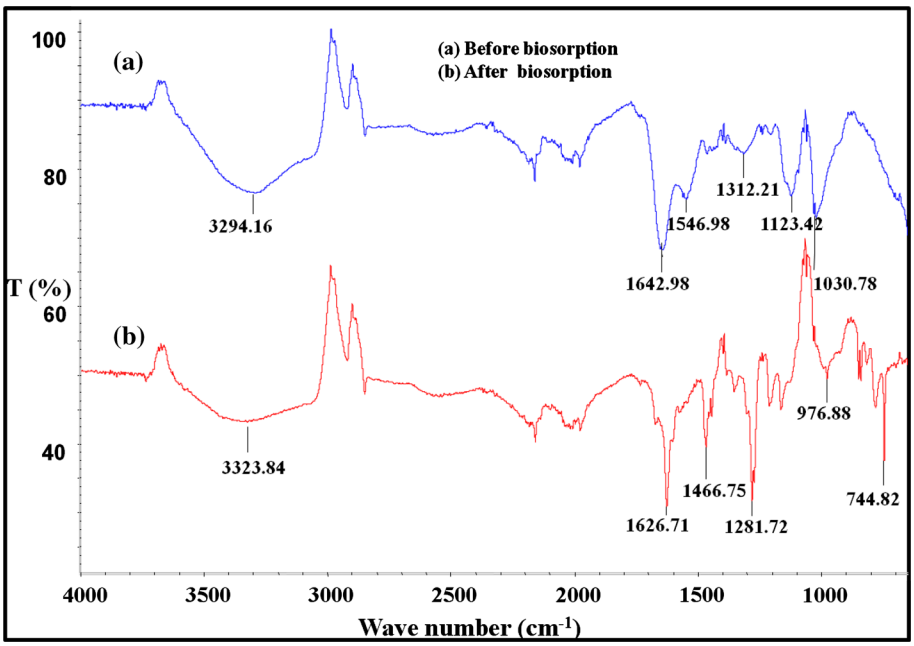


**Fig. 8** FTIR spectra of biomass (**a**) before and (**b**) after adsorption of 1,8-dihydroxy anthraquinone

## Conclusion

The live biomass of *A. oryzae* could be effectively used as a cost-effective adsorbent for the removal of 1,8-dihydroxy anthraquinone from aqueous solution. The live biomass of *A. oryzae* exhibited higher adsorption capacity compared with the dead biomass of *A. oryzae*. Batch adsorption studies showed that the removal rate of 1,8-dihydroxy anthraquinone was highly correlated with the pH, contact time and temperature of adsorption, as well as the initial concentrations of 1,8-dihydroxy anthraquinone and the biomass in aqueous solution. Sorption modeling equation was pseudo-second-order kinetics equation. The experimental equilibrium sorption data under the optimized conditions were well fitted with Langmuir adsorption isotherm equation, exhibiting a monolayer adsorption. The values of dimensionless parameter $R_L$ calculated from the Langmuir constant b were between 0 and 1, suggesting a favorable adsorption. FTIR analysis showed that the surface functional groups were responsible for dye uptake capacity of adsorbents. Taken together, our present study showed that the live biomass of *A. oryzae* could be employed as a low-cost adsorbent to replace commercial activated carbon for the removal of dyes from water and wastewater.

**Acknowledgments** This work was financially supported by the grants from the Scientific and Technological Innovation Projects funds of Jiangsu Province General University Graduate Student (No. CXLX13_687), the National Natural Science Foundation of China (No. 31101269).

## References

Ahmed Basha C, Sendhil J, Selvakumar KV, Muniswaran PKA, Lee CW (2012) Electrochemical degradation of textile dyeing industry effluent in batch and flow reactor system. Desalination 285:188–197

Akar T, Tunali S, Kiran I (2005) *Botrytis cinerea* as a new fungal biosorbent for removal of Pb(II) from aqueous solutions. Biochem Eng J 25:227–235

Akar T, Tosun I, Kaynak Z, Kavas E, Incirkus G, Akar ST (2009) Assessment of the biosorption characteristics of a macro-fungus for the decolorization of Acid Red 44 (AR44) dye. J Hazard Mater 171:865–871

Akkaya G, Özer A (2005) Biosorption of Acid Red 274 (AR 274) on Dicranella varia: determination of equilibrium and kinetic model parameters. Process Biochem 40:3559–3568

Arica MY, Bayramoglu G (2007) Biosorption of reactive Red-120 dye from aqueous solution by native and modified fungus biomass preparations of *Lentinus sajorcaju*. J Hazard Mater 149:499–507

Bhatia S, Sharma DK (2010) Biodesulfurization of dibenzothiophene, its alkylated derivatives and crude oil by a newly isolated strain *Pantoea agglomerans* D23W3. Biochem Eng J 50:104–109

Bhattacharyya KG, Sharma A (2004) Azadirachta indica leaf powder as an effective biosorbent for dyes: a case study with aqueous Congo Red solutions. J Environ Manag 71:217–229

Bosco F, Rugger B, Sassi G (1996) Experimental identification of a scalable reactor configuration for lignin peroxidase production by *Phanerochaete chrysosporiuwl*. J Biotechnol 52:21–39

Carmen Z, Daniela S (2012) Organic pollutants ten years after the Stockholm convention. In: Puzyn T (ed) Environmental and Analytical Update. In Tech, Croatia, pp 55–86

Caro A, Boltes K, Letón P, García-Calvo E (2008) Biodesulfurization of dibenzothiophene by growing cells of *Pseudomonas putida* CECT 5279 in biphasic media. Chemosphere 73:663–669

Chequer FMD, Lizier TM, Felicio R et al (2011) Analyses of the genotoxic and mutagenic potential of the products formed after

the biotransformation of the azo dye Disperse Red. Toxicol In Vitro 25:2054–2063
Chowdhury S, Chakraborty S, Saha P (2011) Biosorption of Basic Green 4 from aqueous solution by *Ananas comosus* (pineapple) leaf powder. Colloid Surface B 84:520–527
Del Río AI, Molina J, Bonastre J, Cases F (2009) Influence of electrochemical reduction and oxidation processes on the decolourisation and degradation of C.I. Reactive Orange 4 solutions. Chemosphere 75:1329–1337
El Haddad M, Regti A, Slimani R, Lazar S (2014) Assessment of the biosorption kinetic and thermodynamic for the removal of safranin dye from aqueous solutions using calcined mussel shells. J Ind Eng Chem 20:717–724
Epolito WJ, Lee YH, Bottomley LA, Pavlostathis SG (2005) Characterization of the textile anthraquinone dye Reactive Blue 4. Dyes Pigm 67:35–46
Ettelaie R, Akinshina A (2014) Colloidal interactions induced by overlap of mixed protein + polysaccharide interfacial layers. Food Hydrocolloids 42:106–117
Freitas AC, Ferreira F, Costa AM et al (2009) Biological treatment of the effluent from a bleached kraft pulp mill using basidiomycete and zygomycete fungi. Sci Total Environ 407:3282–3289
Gulnaz O, Kaya A, Dincer S (2006) The reuse of dried activated sludge for adsorption of reactive dye. J Hazard Mater B134:190–196
Günay A, Arslankaya E, Tosun I (2007) Lead removal from aqueous solution by natural and pretreated clinoptilolite: adsorption equilibrium and kinetics. J Hazard Mater 146:362–371
Gupta VK, Nayak A (2012) Cadmium removal and recovery from aqueous solutions by novel adsorbents prepared from orange peel and $Fe_2O_3$ nanoparticles. Chem Eng J 180:81–90
Gupta VK, Suhas M (2009) Application of low-cost adsorbents for dye removal—a review. J Environ Manag 90:2313–2342
Gupta VK, Gupta B, Rastogi A, Agarwal S, Nayak A (2011a) A comparative investigation on adsorption performances of mesoporous activated carbon prepared from waste rubber tire and activated carbon for a hazardous azo dye—Acid Blue 113. J Hazard Mater 186:891–901
Gupta VK, Jain R, Nayak A, Agarwal S, Shrivastava M (2011b) Removal of the hazardous dye—tartrazine by photodegradation on titanium dioxide surface. Mater Sci Eng C 31:1062–1067
Gupta VK, Jain R, Agarwal S, Nayak A, Shrivastava M (2012) Photodegradation of hazardous dye quinoline yellow catalyzed by $TiO_2$. J Colloid Interface Sci 366:135–140
Gupta VK, Kumar R, Nayak A, Saleh TA, Barakat MA (2013) Adsorptive removal of dyes from aqueous solution onto carbon nanotubes: a review. Adv Colloid Interface Sci 193–194:24–34
Ho YS, McKay G (2000) The kinetics of sorption of divalent metal ions onto sphagnum moss peat. Water Res 34:735–742
Hormiga JA, Vera J, Frías I, Torres Darias NV (2008) Growth and ligninolytic system production dynamics of the *Phanerochaete chrysosporium* fungus: a modelling and optimization approach. J Biotechnol 137:50–58
Hua L, Ma HR, Zhang L (2013) Degradation process analysis of the azo dyes by catalytic wet air oxidation with catalyst CuO/Y-$Al_2O_3$. Chemosphere 90:143–149
Huang Y, Zhang SY, Lv MJ, Xie SG (2010) Biosorption characteristics of ectomycorrhizal fungal mycelium for anthracene 1 adsorption isotherm. Biomed Environ Sci 23:378–383
Ibrahim WM (2011) Biosorption of heavy metal ions from aqueous solution by red macroalgae. J Hazard Mater 192:1827–1835
Iqbal M, Saeed A (2007) Biosorption of reactive dye by loofah sponge-immobilized fungal biomass of *Phanerochaete chrysosporium*. Process Biochem 42:1160–1164
Jain R, Gupta VK, Sikarwar S (2010) Adsorption and desorption studies on hazardous dye Naphthol Yellow S. J Hazard Mater 182:749–756
Kalsoom U, Salman Ashraf S, Meetani MA, Rauf MA, Bhatti HN (2012) Degradation and kinetics of $H_2O_2$ assisted photochemical oxidation of Remazol Turquoise Blue. Chem Eng J 200–202: 373–379
Li WH, Yue QY, Gao BY, Ma ZH, Li YJ, Zhao HX (2011) Preparation and utilization of sludge-based activated carbon for the adsorption of dyes from aqueous solutions. J Chem Eng 171:320–327
Li C, Li Y, Wang J, Cheng J (2013) PA6@FexOy nanofibrous membrane preparation and its strong Cr(VI)-removal performance. J Chem Eng 220:294–301
Lorenc-Grabowska E, Gryglewicz G, Diez MA (2013) Kinetics and equilibrium study of phenol adsorption on nitrogen-enriched activated carbons. Fuel 114:235–243
Marungrueng K, Pavasant P (2007) High performance biosorbent (*Caulerpa lentillifera*) for basic dye removal. Bioresour Technol 98:1567–1572
Meng XM, Liu GF, Zhou JT, Fu QS (2014) Effects of redox mediators on azo dye decolorization by *Shewanella algaeunder* saline conditions. Bioresource Technol 151:63–68
Monash P, Pugazhenthi G (2009) Adsorption of crystal violet dye from aqueous solution using mesoporous materials synthesized at room temperature. Adsorption 15:390–405
Nagy B, Măicăneanu A, Indolean C, Mănzatu C, Silaghi-Dumitrescu L, Majdik C (2013) Comparative study of Cd(II) biosorption on cultivated Agaricus bisporus and wild *Lactarius piperatus* based biocomposites: linear and nonlinear equilibrium modelling and kinetics. J Taiwan Inst Chem Eng. doi:10.1016/j.jtice.2013.08.013
Nasuha N, Hameed BH, Mohd Din AT (2010) Rejected tea as a potential low-cost adsorbent for the removal of methylene blue. J Hazard Mater 175:126–132
Ostolska I, Wiśniewska M (2014) Comparison of the influence of polyaspartic acid and polylysine functional groups on the adsorption at the $Cr_2O_3$—aqueous polymer solution interface. Appl Surf Sci 311:734–739
Pang C, Liu YH, Cao XH, Li M (2011) Biosorption of uranium(VI) from aqueous solution by dead fungal biomass of *Penicillium citrinum*. Chem Eng J 170:1–6
Peng X, Yuan XZ, Zeng GM et al (2014) Synchronous extraction of lignin peroxidase and manganese peroxidase from *Phanerochaete chrysosporium* fermentation broth. Sep Purif Technol 123:164–170
Plazinski W (2013) Binding of heavy metals by algal biosorbents. Theoretical models of kinetics, equilibria and thermodynamics. Adv Colloid Interface Sci 197–198:58–67
Rauf MA, Bukallah SB, Hammour FA, Nasir AS (2008) Adsorption of dyes from aqueous solutions onto sand and their kinetic behavior. Chem Eng J 137:238–243
Ren YX, Nakano K, Nomura M, Chiba N, Nishimura O (2007) A thermodynamic analysis on adsorption of estrogens in activated sludge process. Water Res 41:2341–2348
Saeed A, Iqbal M, Zafar SI (2009) Immobilization of Trichoderma viride for enhanced methylene blue biosorption: batch and column studies. J Hazard Mater 168:406–415
Saeed A, Sharif M, Iqbal M (2010) Application potential of grapefruit peel as dye sorbent: kinetics, equilibrium and mechanism of crystal violet adsorption. J Hazard Mater 179:564–572
Saha PD, Chowdhury S, Mondal M, Sinha K (2012) Biosorption of direct red 28 (Congo Red) from aqueous solutions by eggshells: batch and column studies. Sep Sci Technol 47:112–123
Saratale RG, Saratale GD, Chang JS, Govindwar SP (2011) Bacterial decolorization and degradation of azo dyes: a review. J Taiwan Inst Chem E 42:138–157
Senthil Kumar P, Ramalingam S, Senthamarai C, Niranjanaa M, Vijayalakshmi P, Sivanesan S (2010) Adsorption of dye from aqueous solution by cashew nut shell: studies on equilibrium

isotherm, kinetics and thermodynamics of interactions. Desalination 261:52–60

Shahul Hameed K, Muthirulan P, Meenakshi Sundaram M (2013) Adsorption of chromotrope dye onto activated carbons obtained from the seeds of various plants: equilibrium and kinetics studies. Arab J Chem. doi:10.1016/j.arabjc.2013.07.058

Tamara ZM, Jelena JG, Milovan MS (2015) Surface characterization of mesoporous carbon cryogel and its application in arsenic (III) adsorption from aqueous solutions. Microporous Mesoporous Mater 201:271–276

Tavolaro P, Tavolaro A, Martino G (2009) Influence of zeolite PZC and pH on the immobilization of cytochrome c: a preliminary study regarding the preparation of new biomaterials. Colloids Surf B 70:98–107

Tsantaki E, Velegraki T, Katsaounis A, Mantzavinos D (2012) Anodic oxidation of textile dyehouse effluents on boron-doped diamond electrode. J Hazard Mater 207–208:91–96

Vincent M, Pometto IIIAL, Leeuwen JV (2014) Ethanol production via simultaneous saccharification and fermentation of sodium hydroxide treated corn stover using *Phanerochaete chrysosporium* and *Gloeophyllum trabeum*. Bioresour Technol 158:1–6

Vučurović VM, Radojka RN, Miljić Uroš D, Puškaš VS (2014) Removal of cationic and anionic azo dyes from aqueous solutions by adsorption on maize stem tissue. J Taiwan Inst Chem Eng 45:1700–1708

Wang CP, Sun HW, Liu HB, Wang BL (2014) Biodegradation of pyrene by *Phanerochaete chrysosporium* and enzyme activities in soils: effect of SOM, sterilization and aging. J Environ Sci 26:1135–1144

Xi Y, Shen YF, Yang F, Yang GJ, Liu C, Zhang Z, Zhu DH (2013) Removal of azo dye from aqueous solution by a new biosorbent prepared with *Aspergillus nidulans* cultured in tobacco wastewater. J Taiwan Inst Chem E 44:815–820

Xiao SL, Wang ZJ, Ma H, Yang HJ, Xu WL (2014) Effective removal of dyes from aqueous solution using ultrafine silk fibroin powder. Adv Powder Technol 25:574–581

Zafar SI, Bisma M, Saeed A, Iqbal M (2008) FTIR spectrophotometry, kinetics and adsorption isotherms modeling, and SEM-EDX analysis for describing mechanism of biosorption of the cationic basic dye methylene blue by a new biosorbent (sawdust of silver fir; Abies pind row). Fresen Environ Bull 17:2109–2121

Zeng GM, Zhao MH, Huang DL et al (2013) Purification and biochemical characterization of two extracellular peroxidases from *Phanerochaete chrysosporium* responsible for lignin biodegradation. Int Biodeter Biodegr 85:166–172

Zhang ZC, Liu D, Feng F, Li M, Pang QX, Chen KP (2013) Optimization of the nutrition for biodegradation of vinasse by *Aspergillus oryzae* using response surface methodology. Water Sci Technol 67:772–779

Zhang ZC, Pang QX, Li M, Zheng HH, Chen H, Chen KP (2014) Optimization of the condition for adsorption of gallic acid by Aspergillus oryzae mycelia using Box–Behnken design. Environ Sci Pollut Res. doi:10.1007/s11356-014-3409-3